Revista Mexicana de Astronomía y Astrofísica, **50**, 77–85 (2014)

A SPALLATION MODEL FOR ^{44}TI PRODUCTION IN CORE COLLAPSE SUPERNOVAE

A. Ouyed,[1] R. Ouyed,[1] D. Leahy,[1] and P. Jaikumar[2]

Received 2013 August 11; accepted 2013 December 9

RESUMEN

Los modelos actuales para supernovas con colapso del núcleo (ccSNe) predicen abundancias excesivas de ^{44}Ti comparadas con las observadas. Presentamos un modelo alternativo, en el cual la detonación de una estrella neutrón (Nova Quark o QN) sigue a la explosión de la ccSNe, lo cual tiene como resultado reacciones de espalación en el material arrojado por la SN, que producen ^{44}Ti. Con nuestro modelo y con un retraso adecuado en el tiempo entre la QN y la SN, logramos una producción de ^{44}Ti de $\sim 10^{-4}\ M_{\odot}$. Nuestro modelo también produce señales únicas, que no se encuentran en los modelos estándar de nucleosíntesis en ccSNe. Ejemplos de estas señales son una abundante producción de ^{7}Be y ^{22}Na. Discutimos estas señales mediante el análisis de las curvas de luz tardías y la espectroscopía en rayos gama para nuestro modelo.

ABSTRACT

Current core collapse supernovae (cc-SNe) models predict overproduction of ^{44}Ti compared to observations. We present a model for an alternative channel where a cc-SN explosion is followed by a neutron star detonation (Quark Nova or QN), resulting in a spallation reaction of SN ejecta that produces ^{44}Ti. We can achieve a ^{44}Ti production of $\sim 10^{-4}\ M_{\odot}$ with our model under the right time delay between the QN and the SN. Our model also produces unique signals not found in standard, cc-SN nucleosynthesis models. Some of these unique signals include a significantly large production of ^{7}Be and ^{22}Na. We discuss some of these signals by analyzing the late time light curve and gamma spectroscopy of our model.

Key Words: nuclear reactions, nucleosynthesis, abundances — stars: pre-main sequence — supernovae: general — supernovae: individual (SN1987A, Cassiopeia A)

1. INTRODUCTION

Late time light curves of SNe are considered a relatively accessible resource for studying the nature of SNe, yet, the study of these light curves is ridden with challenges. Very few objects have been studied beyond $\sim$200 days, because as the SN dims out, the dust and the background noise make the signals unreadable (Leibundgut & Suntzeff 2003). Even the most extensively documented supernova, SN1987A, is difficult to study at its later stages, because it is very hard to extrapolate directly the bolometric luminosity after $\sim$1400 days (Leibundgut & Suntzeff 2003). The lack of late time light curve data makes it difficult to formulate standard SN models. SN models have their parameters adjusted so that the isotopic yields reflect the abundances inferred from late time light curves (Limongi & Chieffi 2006), which makes them dependent on the quality and understanding of our current observations. An example of the problematic nature of standard core collapse SN models, is ^{44}Ti production. Although ^{44}Ti production is assumed to be universal in cc-SNe models (The et al. 2006; Woosley, Langer, & Weaver 1995), only SN1987A is documented well enough to be able to extrapolate

[1]University of Calgary, Canada.
[2]California State University, Long Beach, USA.

^{44}Ti from the bolometric light curve. The problem is accentuated by the fact that current telescopes have only been able to detect ^{44}Ti decay lines in Cassiopeia A (The et al. 2006), and recently in SN1987A (Grebenev et al. 2012), whereas current models predict more detections (The et al. 2006).

In this paper, we attempt to solve some of these problems by proposing an alternative channel to the standard cc-SN model. After the SN explosion, neutron stars that undergo an evolution (e.g. matter fallback, or spin-down) towards quark deconfinement densities will transition to a lower energy, strange matter phase and experience an energetic detonation (Quark Nova or QN; Ouyed, Dey, & Dey 2002). The neutron star will release its outer layers as relativistic, neutron rich ejecta (Keränen, Ouyed, & Jaikumar 2005; Ouyed, Rapp, & Vogt 2005; Niebergal, Ouyed, & Jaikumar 2010), where the ejecta interact with the SN envelope (dual-shock Quark Nova, or dsQN). The time delay (hereafter $t_{\rm delay}$) between the two detonations constrains the nature of the interaction, where a time delay on the order of days will cause significant spallation of SN ejecta by QN neutrons. The spallation reaction creates unique signals in the late time light curve which are due to the modification of radioactive isotope abundances. The time delay $t_{\rm delay}$ between the QN and SN detonations acts as a parameter for the isotopic abundances. The different abundances of isotopes will also create specific γ spectroscopic signals. Currently, there have been many indirect observations for QN suggested (e.g. Hwang & Laming 2012; Ouyed et al. 2012; Leahy & Ouyed 2008; Ouyed 2013a; Ouyed & Leahy 2013).

In continuation to Ouyed et al. (2011), we explain the ^{44}Ti synthesis measured in the late-time light curves of cc-SNe (Woosley & Hoffman 1991) as a product of nuclear spallation from the dsQN, in contrast to the traditional view that it is produced by the SN *in situ*. The conditions necessary for the production of a QN, and the constraints set by the parameter $t_{\rm delay}$, explain the rarity of observations of ^{44}Ti nuclear decay lines. In contrast to our earlier paper (Ouyed et al. 2011), we avoid excessive destruction of ^{56}Ni by spallation, by taking into account the mixing of the SN's layers. Current observations seem to support the picture of mixing (Mueller, Fryxell, & Arnett 1991). Furthermore, numerical studies have shown that Rayleigh Taylor instabilities can cause considerable mixing in a very short time span (Kifonidis et al. 2000; Hachisu et al. 1991; Mueller et al. 1991). If ^{56}Ni is mixed through the SN envelope, there are less ^{56}Ni atoms in the inner layer. This would lead to QN neutrons hitting less ^{56}Ni, as opposed to the picture where all ^{56}Ni is concentrated in the inner layers (Ouyed et al. 2011). By avoiding excessive nickel depletion, we can avoid the sub-luminosity characteristic in Ouyed et al. (2011).

2. MODEL

We extend the model we presented in Ouyed et al. (2011) by including mixing. In analogy to lab terminology, we divide our model into a beam part and a target part. The scenario consists of a beam of relativistic QN ejecta that collides with a target, that is, the expanding, inner layers of the SN envelope. The time delay between the SN denotation and neutron star detonation and the mixing of the SN ejecta are the key parameters in our model.

2.1. *Beam*

In past studies (Keränen et al. 2005; Ouyed et al. 2005; Niebergal et al. 2010), the authors explored the explosion mechanism of the neutron star and the dynamics of the QN ejecta. A neutron star can detonate through an explosive conversion into a quark star and eject its outermost layers as a mass of $M_{\rm QN} \sim 10^{-3}\,M_\odot$. We can model the QN ejecta as a pulse of $N^0 \sim 1.2 \times 10^{54} M_{\rm QN,-3}$ neutrons where $M_{\rm QN,-3}$ means $M_{\rm QN}$ in units of $10^{-3}\,M_\odot$. The neutrons are relativistic, with an energy of ∼10 GeV (Ouyed et al. 2011).

2.2. *Target*

We model the target as an expanding SN envelope of inner radius $R = v_{\rm SN} t_{\rm delay}$, where $v_{\rm SN} = 5000$ km s^{-1} is the velocity of the SN ejecta, and $t_{\rm delay}$ is the time delay between the neutron star detonation and the SN detonation. We assume the exploding star is $\sim 20\,M_\odot$. In contrast to the original model (Ouyed et al. 2011), we assume different degrees of mixing. The target is the inner layers of the expanding SN envelope, which are composed of ^{16}O,^{12}C, and ^{56}Ni, whether these isotopes are stratified into separate layers or mixed. We assume

that the whole SN envelope has a total ^{56}Ni mass of $\sim 0.1\,M_\odot$, and O and C have total masses of $\sim 1.0\,M_\odot$ each (Ouyed 2013a). We treat a target number density n as constant, with

$$n = n_{\rm Ni} + n_{\rm O} + n_{\rm C} = \frac{N}{4\pi R^2 \Delta R}, \tag{1}$$

where ΔR is the thickness containing a layer and N is total number of atoms within ΔR. Our mean free path λ is

$$\lambda = \frac{1}{n_{\rm Ni}\sigma_{56} + n_{\rm C}\sigma_{12} + n_{\rm O}\sigma_{16}}, \tag{2}$$

where we use the semi-empirical cross section $\sigma_A = 45$ mb $\times A^{0.7}$ (Letaw, Silberberg, & Tsao 1983), where A is mass number. For our model, we use equations (1) and (2) to divide the thickness ΔR into $N_{\rm coll}$ imaginary layers of width λ,

$$N_{\rm coll} = \frac{\Delta R}{\lambda} \approx 57.54\,\frac{(M_{\rm Ni,0.1\,M_\odot}/56^{0.3}) + (M_{\rm O,0.1\,M_\odot}/16^{0.3}) + (M_{\rm C,0.1\,M_\odot}/12^{0.3})}{\left(v_{\rm SN,1000km/s} \times t_{\rm delay,10\,days}\right)^2}, \tag{3}$$

where $N_{\rm coll}$ represents the number of collisions an incoming neutron with ΔR. The subscript indicates the units, for example, $M_{\rm O,0.1\,M_\odot}$ is in units of $0.1\,M_\odot$. The interaction of that neutron with a SN atom will release a multiplicity ζ of nucleons,

$$\overline{\zeta}(E, A) \approx 4.67 A_{56}(1 + 0.38\,\ln E) Y_{\rm np}, \tag{4}$$

where E stands for neutron energy in MeV, A_{56} is atomic mass number of target divided by 56, and $1.25 < Y_{\rm np} < 1.67$ (Cugnon, Volant, & Vuillier 1997; Ouyed et al. 2011).

2.3. *Spallation Statistics*

At each layer k of radial thickness λ, an atom will be bombarded by $N^0_{\rm hits}$ neutrons, resulting in the nucleus (Ouyed et al. 2011),

$$A^{N^0_{\rm hits}} = A^0 - \sum_{j=0}^{N^0_{\rm hits}-1} \zeta^0(E^0, A^j). \tag{5}$$

The amount of neutrons that hit a particular isotope species i is statistically weighted by the ratio of that isotope nuclei i over the total nuclei present in that target.

$N^0_{\rm hits}$ is drawn from a Poisson distribution that peaks at,

$$\overline{N}^0_{\rm hits} \sim \left(\frac{N_{\rm Ni}\sigma_{\rm Ni} + N_{\rm C}\sigma_{\rm C} + N_{\rm O}\sigma_{\rm O}}{N_{\rm Ni} + N_{\rm C} + N_{\rm O}}\right)\left(\frac{N^0(1 - e^{-1})}{4\pi R^2}\right), \tag{6}$$

where N_i is the number of atoms of isotope i, and σ_i is the spallation cross section for isotope i. ζ^0 is drawn from a Poisson distribution that peaks at equation (4).

For subsequent layers, it follows that

$$\overline{N}^k_{\rm hits} = (1 - e^{-1})\overline{\zeta}^k \overline{N}^{k-1}_{\rm hits}\ , \tag{7}$$

and the mean nucleon energy for each subsequent layer is,

$$E^k \sim \frac{E^{k-1}}{\overline{\zeta}^{k-1}}\ , \tag{8}$$

where spallation ceases at an energy of $E \sim 73$ MeV (Cugnon et al. 1997).

2.4. *Mixing*

The isotope production in our model strongly depends on the nature of the mixing in the target. We therefore define mixing as a parameter, where an unmixed state and a total mixed state form the two most extreme values of the parameter. Furthermore, we use a third "half-mixed" state, that lies between the two extremes. For simplicity, we assume that the angular distribution of each isotope species is relatively homogenous in the inner layers, so equation (1) applies. In the model, the unmixed state follows an onion layer profile, where the target is stratified into layers and each layer is made of a specific isotope. In our case, there is the innermost layer made of $M_{\rm Ni} = 0.1\,M_\odot$, followed by a second layer of $M_{\rm O} = 1.0\,M_\odot$, and a third layer of $M_{\rm C} = 1.0\,M_\odot$. The half-mixed state is still stratified into layers, but the ^{56}Ni layer is contaminated by O, and the O layer is contaminated by a small amount ^{56}Ni, and the C layer remains pristine. So, for the half-mixed state, the first layer consists of $M_{\rm Ni} = 0.05\,M_\odot$ and $M_{\rm O} = 0.05\,M_\odot$, the second layer of $M_{\rm Ni} = 0.05\,M_\odot$ and $M_{\rm O} = 0.95\,M_\odot$, and the third layer of $M_{\rm C} = 1.0\,M_\odot$. We define the total mixed state as a state where the mixing has spread the total mass of each of the original isotopes homogeneously through the entire envelope, effectively destroying layer stratification. The masses of an an inner, mixed $1.0\,M_\odot$ target then become $M_{\rm Ni} = 0.0476\,M_\odot$, and $M_{\rm O} = M_{\rm C} = 0.476\,M_\odot$. In the case of the totally mixed state, we treat the SN envelope as one layer with equation (1), where the layer contains the mixed ^{56}Ni,O and C.

2.5. *Light Curve Model*

We compute the late time light curve by extending our spallation code with the Supernova Light Curves' Code for Cococubed program[3]. Our spallation code computes the mass yields of different isotopes using the model in § 2, and the Cococubed extension computes the bolometric luminosity from the isotope mass yields. We also take into account the contributions of ^{57}Ni, and ^{60}Co to the bolometric light curve, and we take their mass values from Woosley et al. (1995). In our model, we assume the simple case where the bolometric luminosity is entirely caused by the thermalization of nuclear decay radiation.

3. RESULTS

3.1. *Photometry*

The key isotopes for the light curve (Figure 1) are ^{56}Ni and ^{44}Ti. In Figure 2, we notice that the luminosity of the first ∼1000 days strongly depends on mixing. This is because the amount of mixing dictates how much ^{56}Ni is available in the inner layers as target for QN neutrons. In the first ∼1000 days the ^{56}Ni decay radiation dominates the bolometric luminosity. Mixing transports nickel into the outer shells, so if mixing increases, less nickel is available in the inner layers to be destroyed by energetic neutrons. An unmixed target experiences the most destruction of ^{56}Ni, which translates into a lower luminosity in the first days of the light curve. In Ouyed et al. (2011) we explored an unmixed dsQN as a possible candidate for Cassiopeia A. We argued that an unmixed dsQN was a plausible candidate because the sub-luminosity caused by ^{56}Ni depletion correlated with Flamsteed's sub-luminous observation, and the ^{44}Ti synthesis caused by ^{56}N spallation correlated with COMPTEL's and BEPPO SAX's ^{44}Ti detection (Iyudin et al. 1994; Ouyed et al. 2011).

We notice that the luminosity is less strongly affected by the mixing after ~ 1000 days. This weaker dependence is due to the fact that ^{44}Ti synthesis does not seem to change much across mixing space. Even if ^{44}Ti does vary across the different mixed states, the order of magnitude $M_{\rm Ti} \sim 10^{-4}\,M_\odot$ stays the same.

For $t_{\rm delay} = 4$ days, and total mixing, our model synthesized $\sim 10^{-4}\,M_\odot$ of ^{44}Ti, which compares favorably to the amounts found by γ-ray telescopes in Cassiopeia A (Iyudin et al. 1994), amounts estimated from the light curve of SN1987A (Suntzeff et al. 1992; Woosley & Hoffman 1991), and the amount detected with INTEGRAL (Grebenev et al. 2012). Furthermore, we notice there is very little nickel that is depleted − indeed most of the original inner $0.0476\,M_\odot$ is maintained for 3 days $\leq t_{\rm delay} \leq 10$ days. If very little ^{56}Ni is depleted from the inner mass, then the total $\sim 0.1\,M_\odot$ for ^{56}Ni that is spread throughout the whole envelope is more or less maintained throughout different time delays. The $\sim 0.1\,M_\odot$ mass for ^{56}Ni compares quite well with what is observed in type II SN light curves (Suntzeff et al. 1992; Woosley & Hoffman 1991). Another interesting

[3]Code by F. X. Timmes, `http://cococubed.asu.edu/code_pages/snlite.shtml`.

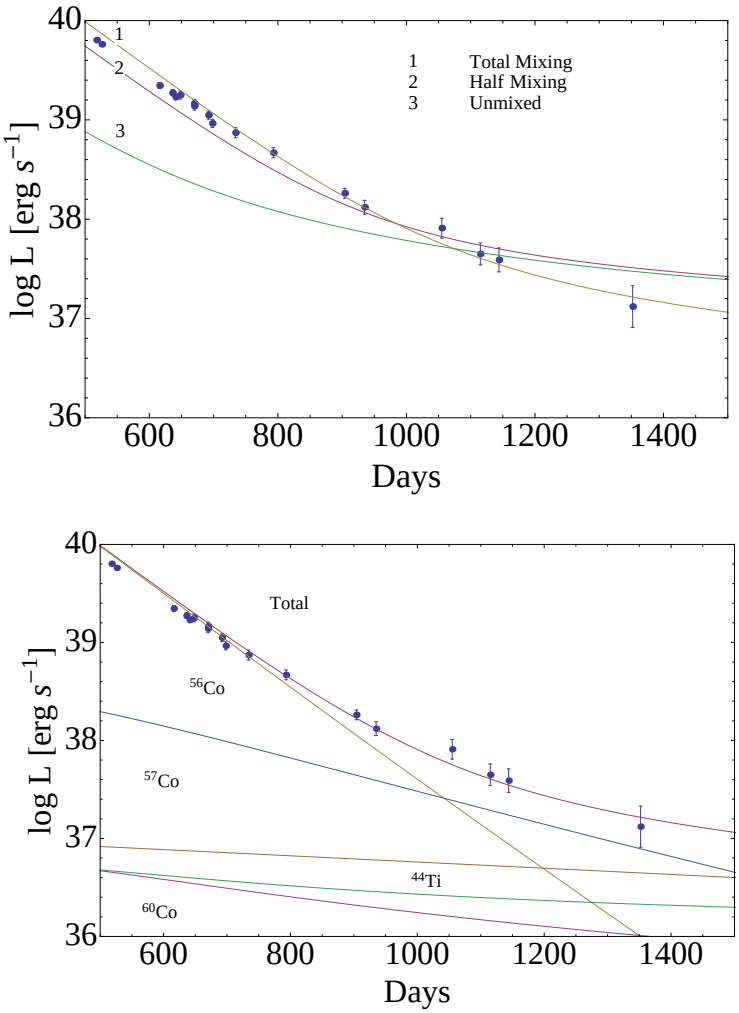

Fig. 1. The SN1987A data comes from Suntzeff et al. (1991). The time delays represented in the upper panel are $t_{\rm delay} = 3, 4$ and 9 days. In the upper panel we also depict the original $M_{\rm Ni} = 0.1\,M_\odot$ target without the spallation, where luminosity contributions of ^{57}Co and ^{60}Co were added artificially, and their values, $5.5 \times 10^{-3}\,M_\odot$ and $1.14 \times 10^{-5}\,M_\odot$, respectively, were taken from Woosley et al. (1995). The points are the SN 1987A data and the solid lines indicate our model. The y-axis is the logarithm of luminosity in units of erg s^{-1}. In the lower plot, we also include the individual luminosity contributions of each isotope, where the contributions of ^{57}Co and ^{60}Co were artificially constructed in identical fashion to the upper panel. The masses of ^{56}Ni, ^{22}Na and ^{44}Ti, are actual, spallation products of our model. For $t_{\rm delay} = 4$ days, the values are $0.99\,M_\odot$, $5.50 \times 10^{-5}\,M_\odot$, and $1.20 \times 10^{-4}\,M_\odot$, respectively. The color figure can be viewed online.

isotope is ^{22}Na, and it is synthesized at a high amount of almost $\sim 10^{-4}\,M_\odot$ which contrasts with the estimates of $\sim 10^{-6}\,M_\odot$ (Woosley et al. 1995). This creates a contribution to the bolometric luminosity higher than normally expected. We see in the upper panel of Figure 1 a dependence of the light curve on $t_{\rm delay}$. We can see that later stages of the late time light curve are the most visibly affected by the time delay. This strong dependence in the later days is modulated by the production of ^{44}Ti, because ^{44}Ti yields are much affected by the time delay (Figure 3). The earlier days of the late time light curve seem to be affected only weakly by the time delay change, because ^{56}Ni destruction stays more or less constant (Figure 3). This weak dependence of ^{56}Ni to $t_{\rm delay}$, at least for the total mixed state, is interesting because ^{56}Ni varies substantially across mixing space. In contrast, we find that for the total mixed state, ^{44}Ti production depends strongly on $t_{\rm delay}$. but it varies very weakly across mixing space.

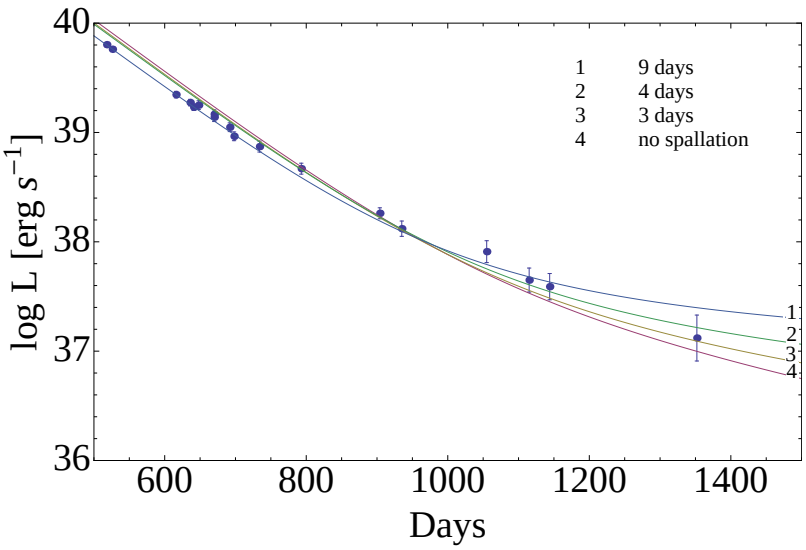

Fig. 2. Light curves of our model at $t_{\rm delay} = 4$ days for different mixing states and the SN1987A data. The SN1987A data comes from Suntzeff et al. (1991) and is plotted for reference. The points are the SN 1987A data and the solid lines indicate our model. The y-axis is the logarithm of luminosity in units of erg s^{-1}. The color figure can be viewed online.

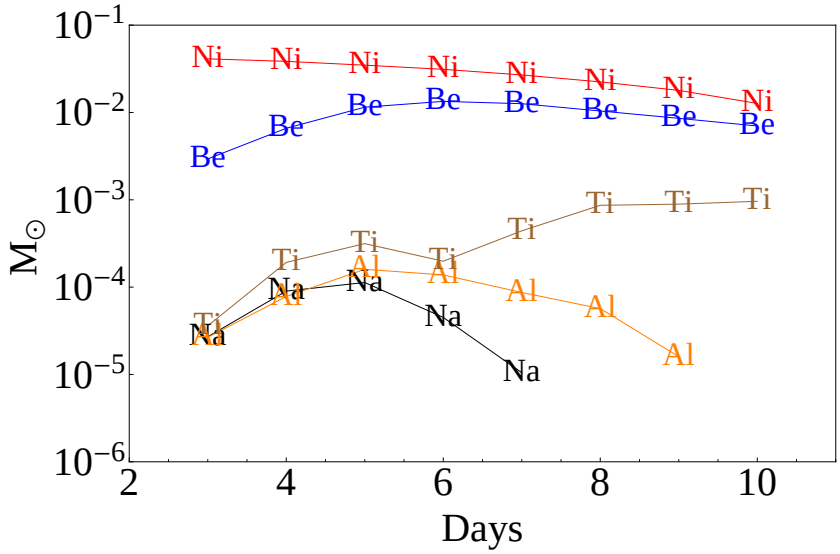

Fig. 3. Mass yields of ^{56}Ni, ^{44}Ti, ^{22}Na, ^{26}Al and ^{7}Be, where x-axis represents $t_{\rm delay}$ and the y-axis represents the mass in units of $M_\odot$. The panel depicts the yields for spallation of the inner $\sim 1.0\,M_\odot$ of the SN ejecta. The color figure can be viewed online.

3.2. *Isotope Abundance*

Our spallation model creates isotopes of almost every mass number in the range of $A < 56$. However, very few of the isotopes created can be detected with γ-ray telescopes, because the SN envelope only becomes transparent to nuclear decay radiation after a time period of at least months (Diehl 2012), so only isotopes that have a half life of at least of the order of weeks will have detectable nuclear decay lines. Therefore, in Figure 3, we only include the masses of isotopes with half lives of at least of the order of weeks.

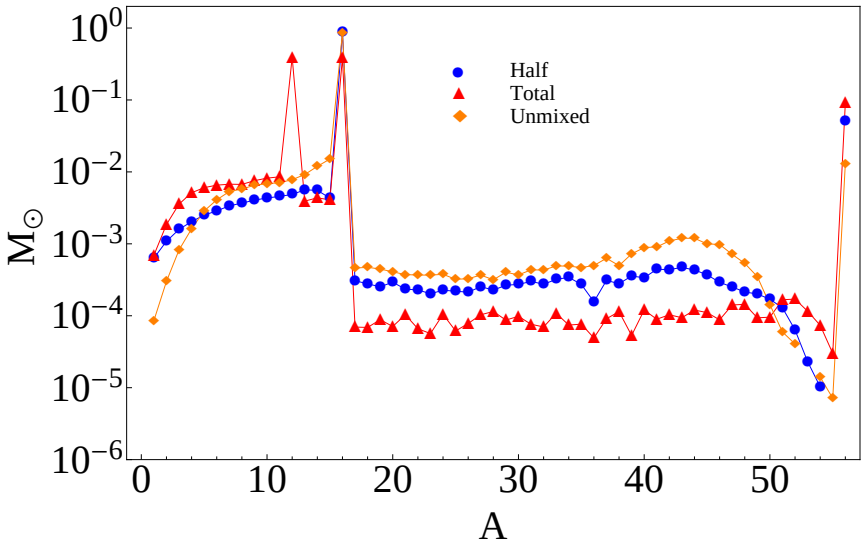

Fig. 4. Mass in $M_\odot$ of isotopes of a particular atomic mass number produced by our spallation model at a $t_{\rm delay} = 4$ days, for the three different mixed states. The x-axis represents the mass number A, and the y-axis represents the mass of nucleus of mass number A. The color figure can be viewed online.

In Figures 3 and 4 we plot some of the trends of these isotopes. We notice that in Figure 4, the model produces more mass for light isotopes than heavier isotopes. This is caused by the spallation of C and O. We also notice that the plots in Figure 4 are divided in roughly two plateaus, with their boundary at $A \sim 16$, which is the atomic mass number of oxygen. We observe that for $A < 6$, the unmixed target produces the least amount of mass. Spallation of C and O enhances the production of light isotopes, yet, in the unmixed state, O and C are shielded by the Ni layer. Therefore, only spallation neutrons that manage to traverse the Ni layer will be able to interact with the O layer (At $t_{\rm delay} = 4$ days spallation neutrons do not reach the C layer in the unmixed state). We also notice that the two sides divided by $A \sim 16$ represent opposing trends. In $A < 16$, the totally mixed state produces the most mass, while sometimes the half-mixed state produces more mass than the unmixed state, and viceversa. Yet, at $A > 16$, the unmixed state produces the most mass, followed by the half-mixed, with the mixed state producing the least mass. This hierarchy of production at $A > 16$ is created by the availability of ^{56}Ni for spallation neutrons. The more mixing the target experiences, the least amount of ^{56}Ni is spallated, and therefore the least amount of heavier isotopes is created. In Figure 3, which represents the mass trends for a totally mixed state, we plot the mass of one of the lighter isotopes, ^{7}Be, which has a half life of 76 days, which gives enough time for nuclear decay photons to go through the SN photosphere. Compared to the models of Woosley et al. (1995), we notice that our model produces more ^{7}Be and ^{22}Na. We also notice that ^{44}Ti, ^{56}Ni, and ^{26}Al are of the same order of magnitudes as in other models (Woosley et al. 1995). Finally, it seems we can constrain the production of ^{22}Na and ^{26}Al at higher $t_{\rm delay}$, since ^{22}Na production ends at $t_{\rm delay} \sim 7$ and ^{26}Al production at $t_{\rm delay} \sim 8$ days.

4. DISCUSSION AND PREDICTIONS

- *^{44}Ti production as a dsQN specificity and SN1987A:* We argue that the rarity of observations (The et al. 2006) of ^{44}Ti might be related to the fact that ^{44}Ti is not produced by standard cc-SNe, but by dsQNe. In a recent paper (Ouyed et al. 2011) we argued that CasA's ^{44}Ti lines were produced by a an unmixed dsQN through a significant ^{56}Ni depletion. Although it is probably possible to avoid the excessive ^{56}Ni depletion in our original model by adjusting some parameters, and yet still predict a ^{44}Ti mass yield that is compatible with observations, it seems more natural and elegant to extend our model with mixing. Through total mixing, we can predict very minimal destruction of ^{56}Ni (Figure 3) because ^{56}Ni is spread throughout the whole envelope as opposed to the assumption where it is all concentrated

in the inner layers. If ^{56}Ni is spread throughout a wider volume, then fewer ^{56}Ni atoms will be available in the inner layers as targets for QN neutrons. This minimal depletion leaves almost all the $\sim 0.1\,M_{\odot}$ of ^{56}Ni intact. In Figure 1 we plotted the data of SN1987A against our model; SN1987A is a SN where ^{44}Ti has been measured indirectly (Motizuki & Kumagai 2004; Suntzeff et al. 1992; Woosley & Hoffman 1991) and recently directly (Grebenev et al. 2012). At lower time delays, QN energy is mostly spent in PdV work (Leahy & Ouyed 2008); therefore, at a time delay of 4 days, our model could reproduce a similar luminosity to SN1987A. Current observations of SN1987A point to thorough mixing of SN layers (Mueller et al. 1991), which compares well to the assumptions about mixing done in our model. Although a traditional, non-spallation model for SN1987A provides a good fit for the light curve, the traditional model fails to account for the apparent sub-luminosity of CasA (Ouyed et al. 2011), whereas both CasA and SN1987A have similar amounts of ^{44}Ti. This discrepancy in our model is explained through the fact that CasA can possibly be an unmixed dsQN, and SN1987A-like objects mixed dsQNs. Recent papers have provided alternative arguments for the possibility of SN1987A compact remnant being a Quark Star (Chan et al. 2009).

- *^{7}Be abundance:* In Figures 3 and 4, across all mixing space, a very large abundance of ^{7}Be is produced compared to current cc-SN models (Diehl & Timmes 1998; Woosley et al. 1995). Current core collapse SN models do not produce enough ^{7}Be to reach the photosphere before ^{7}Be decays. However, our model predicts $\sim 10^{-3} - 10^{-2}\,M_{\odot}$ for ^{7}Be, which could be enough so that a significant amount of it reaches the photosphere and therefore may be detected by γ-ray telescopes. The 487 keV photon released by the β-decay of ^{7}Be into ^{7}Li, is in the detectable energy range of current γ-ray telescopes (INTEGRAL, NuSTAR, etc.). The large abundance of ^{7}Be is due to the spallation of mixed O and C in the inner SN layers. This high abundance in our model indicates that only core collapse SN that evolve into dsQN will have a detectable gamma signature of ^{7}Be. Currently, novae are the only possible sources of detectable ^{7}Be photons because standard cc-SN are too optically thick (Diehl & Timmes 1998). However our dsQN model can produce an alternative point source of ^{7}Be photons. Our model produces significant amounts of ^{7}Be across the three mixed states (Figure 4). Finally, such a massive amount of ^{7}Be should create a signature in the bolometric light curve. If we assume Cassiopeia A was an unmixed dsQN (Ouyed et al. 2011), it should have emitted a ^{7}Be signature shortly after detonation.

- *^{22}Na abundance:* A small ^{22}Na contribution is predicted in late time core collapse SN light curves (Woosley et al. 1995). However, our spallation model generates a much larger amount of ^{22}Na than expected. This large yields of ^{22}Na are due to the spallation of ^{56}Ni into lighter nuclei. Current models (Woosley et al. 1995) give a $\sim 10^{-6}\,M_{\odot}$ for ^{22}Na, while our spallation model can produce as much as $\sim 10^{-3}\,M_{\odot}$ (Figure 4). Furthermore, ^{22}Na has a half-life of 2.6 yr, and decays into an excited state of ^{22}Ne, releasing energetic radiation (Diehl & Timmes 1998). This large amount generates enough radiation to create a noticeable signal in the late time light curve, as pictured in Figure 1. The decay of ^{22}Na emits a 1.275 MeV γ line that can be detected by current γ-ray telescopes. These signals of ^{22}Na abundant dsQN cannot be reproduced in current models for cc-SNe.

- *Some limitations of our model:* Some simplifications were made in our model. One of them concerns the structure of the SN ejecta. Here, we only include O, C and ^{56}Ni as targets (See, however Ouyed 2013b). Furthermore, O, C, and ^{56}Ni spread isotropically across space. This isotropic distribution allows us to model the spallation targets with statistical weights derived from the isotopic abundances. However, studies of CasA's remnants point to asymmetry in the detonation (e.g. Fesen et al. 2006).
  Moreover, the calculation for $N^{0}_{\rm hits}$, the number of projectile neutrons that hit a target isotope, is simplified. In equation (6), the number of hits is a function of the initial target isotopes and their cross-sections. However, in equation (5), the target isotopes are transformed into different daughter isotopes after each neutron hit. If the target nuclei change, their cross-sections should change after each neutron hit as well. In a more realistic model, this change of cross section would be taken into account. However, our current model does not take into account this change of target nuclei in the calculation for $N^{0}_{\rm hits}$.
  Another simplification is related to the nuclear processes in the SN ejecta. We did not touch upon nuclear electron capture, neutrino capture, and other nuclear decay processes. These processes might affect the Ti and Ni channels.

While a a different method for discretizing the spallation reactions might yield some differences, the broad trends explored in our model will remain. These broad trends, that ^{44}Ti can be produced from a minimal destruction of ^{56}Ni, that spallation of ^{56}Ni will lead to enrichment of ^{22}Na, and that spallation of O, and C will lead to an excess of ^{7}Be, seem reasonable. Furthermore, ^{56}Ni that is transported into the outer layers by a mixing mechanism would experience less spallation than inner layer ^{56}Ni − thus creating the possibility for either sub-luminous or non sub-luminous Ti-rich objects. While other limitations of our model exist, which are discussed in Ouyed et al. (2011), the model contains testable predictions for ^{22}Na and ^{7}Be enrichment.

This research is supported by an operating grant from the National Science and Engineering Research Council of Canada (NSERC). We also thank N. Koning and M. Kostka for helpful discussions.

REFERENCES

Chan, T. C., Cheng, K. S., Harko, T., Lau, H. K., Lin, L. M., Suen, W. M., & Tian, X. L. 2009, Apj, 695, 732
Cugnon, J., Volant, C., & Vuillier, S. 1997, Nuclear Physics A, 625, 729
Diehl, R. 2012, arXiv:1202.0481 [astro-ph.HE]
Diehl, R., & Timmes, F. 1998, PASP, 110, 637
Fesen, R. A., et al. 2006, ApJ, 645, 283
Grebenev, S. A., Lutovinov, A. A., Tsygankov, S. S., & Winkler, C. 2012, Nature, 490, 373
Hachisu, I., Matsuda, T., Nomoto, K., & Shigeyama, T. 1991, ApJ, 368, L27
Hwang, U., & Laming, J. M. 2012, ApJ, 746, 130
Iyudin, A., et al. 1994, A&A, 284, L1
Keränen, P., Ouyed, R., & Jaikumar, P. 2005, ApJ, 618, 485
Kifonidis, K., Plewa, T., Janka, H.-Th., & Müller, E. 2000, ApJ, 531, L123
Leahy, D., & Ouyed, R. 2008, MNRAS, 387, 1193
Leibundgut, B., & Suntzeff, N. 2003, Lect. Notes Phys., 598, 77
Letaw, J. R., Silberberg, R., & Tsao, C. H. 1983, ApJS, 51, 271
Limongi, M., & Chieffi, A. 2006, in AIP Conf. Proc. 847, Origin of Matter and Evolution of Galaxies, ed. S. Kubono, W. Aoki, T. Kajino, T. Motobayashi, & K. Nomoto (New York: AIP), 99
Motizuki, Y., & Kumagai, S. 2004, in AIP Conf. Proc. 704, Tours Symposium on Nuclear Physics V, ed. M. Arnould, M. Lewitowicz, G. Münzenberg, H. Akimune, M. Ohta, H. Utsunomiya, T. Wada, & T. Yamagata (New York: AIP), 369
Mueller, E., Fryxell, B., & Arnett, D. 1991, A&A, 251, 505
Niebergal, B., Ouyed, R., & Jaikumar, P. 2010, Phys. Rev. C, 82, id. 062801
Ouyed, R. 2013a, MNRAS, 428, 236
_____. 2013b, arXiv:1304.3715
Ouyed, R., Dey, J., & Dey, M. 2002, A&A, 390, L39
Ouyed, R., Kostka, M., Koning, N., Leahy, D. A., & Steffen, W. 2012, MNRAS, 423, 1652
Ouyed, R., & Leahy, D. 2013, Res. Astron. Astrophys., 13, 1202
Ouyed, R., Leahy, D., Ouyed, A., & Jaikumar, P. 2011, Phys. Rev. Lett., 107, id. 151103
Ouyed, R., Rapp, R., & Vogt, C. 2005, ApJ, 632, 1001
Suntzeff, N. B., Phillips, M. M., Depoy, D. L., Elias, J. H., & Walker, A. R. 1991, AJ, 102, 1118
Suntzeff, N. B., Phillips, M. M., Elias, J. H., Walker, A. R., & Depoy, D. L. 1992, ApJ, 384, L33
The, L.-S., Clayton, D. D., Diehl, R., Hartmann, D. H., Iyudin, A. F., Leising, M. D., Meyer, B. S., Motizuki, Y., & Schönfelder, V. 2006, A&A, 450, 1037
Woosley, S. E., & Hoffman, R. D. 1991, ApJ, 368, L31
Woosley, S. E., Langer, N., & Weaver, T. A. 1995, ApJ, 448, 315

Denis Leahy, Amir Ouyed, and Rachid Ouyed: Department of Physics and Astronomy, University of Calgary, 2500 University Drive NW, Calgary, Alberta, T2N 1N4 Canada (leahy, ahouyedh, rouyed@ucalgary.ca).
Prashanth Jaikumar: Department of Physics and Astronomy, California State University, Long Beach, 1250 Bellflower Blvd., Long Beach, CA 90840, USA (Prashanth.Jaikumar@csulb.edu).